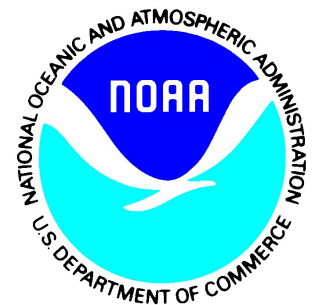


---

NOAA/NESDIS/STAR

**Algorithm and Theoretical  
Basis Document for  
the NOAA Oceansat-3 (EOS-06)  
Scatterometer Data Products**

*Compiled by the*  
**Ocean Surface Winds Science Team**



**Version 1.0**  
**December 10, 2024**

---

TITLE: ALGORITHM AND THEORETICAL BASIS DOCUMENT FOR THE NOAA  
OCEANSAT-3 (EOS-06) SCATTEROMETER DATA PRODUCTS VERSION 1.0

AUTHORS:

Seubson Soisuvam (UCAR)

Zorana Jelenak (UCAR)

Paul S. Chang (NOAA/NESDIS/STAR)

## DOCUMENT HISTORY DOCUMENT REVISION LOG

The Document Revision Log identifies the series of revisions to this document since the baseline release. Please refer to the above page for version number information.

<b>DOCUMENT TITLE: Algorithm and Theoretical Basis Document for the NOAA Oceansat-3 (EOS-06) Scatterometer Data Products</b>			
<b>DOCUMENT CHANGE HISTORY</b>			
<b>Revision No.</b>	<b>Date</b>	<b>Revision Originator Project Group</b>	<b>CCR Approval # and Date</b>
1.0	Dec. 2024	N/A	N/A

## LIST OF CHANGES

Significant alterations made to this document are annotated in the List of Changes table.

<b>DOCUMENT TITLE: Algorithm and Theoretical Basis Document for the NOAA Oceansat-3 (EOS-06) Scatterometer Data Products</b>
--



3. LEVEL-2A (L2A).....	12
3.1. Grid Cell Generation.....	12
3.2. Sigma0 Grouping.....	15
3.3. Row Time .....	18
4. LEVEL-2B (L2B).....	20
4.1. Preprocessing.....	20
4.1.1. Sigma0 Calibration.....	21
4.2. Wind Inversion.....	22
4.2.1. Geophysical Model Function.....	23
4.2.2. Solution Ranking.....	23
4.3. Ambiguity Removal.....	24
4.4. Rain-impacted Wind Retrievals.....	28
4.4.1. Rain Rate and Rain Flag.....	29
4.5. Quality Control.....	31
5. REFERENCES.....	33
6. APPENDIX A.....	35
7. APPENDIX B.....	37

## LIST OF FIGURES

	<u>Page</u>
Figure 1-1 OSCAT-3 Measurement Geometry. ....	9
Figure 3-1. L2A row and cell index generation. ....	15
Figure 3-2. Sigma0 compositing scheme. ....	16

Figure 3-3. Sigma0 slice composite counts per 12.5 km WVC. ....	17
Figure 3-4. Slice composite of four-flavors sigma0. ....	18
Figure 4-1. Changes in sigma0 calibration values over time. ....	22
Figure 4-2. Ambiguity removal scheme. ....	24
Figure 4-3. Changes in brightness temperature values over time. ....	28
Figure 4-4. OSCAT-3 rain rates and rain impact on wind speed performance. ....	29

## LIST OF TABLES

	<u>Page</u>
Table 1-1. OSCAT-3 Specifications.....	10
Table 6-1. List of L2A HDF5 variables .....	34
Table 6-2. List of L2B NetCDF variables .....	35
Table 7-1. L2A quality control flag. ....	36
Table 7-2. L2B quality control flag. ....	37

## 1. INTRODUCTION

## 1.1. About this Document

This document describes the algorithm for the Oceansat-3 (EOS-06) Scatterometer, also known as the OSCAT-3, data products developed by the Ocean Surface Winds Team at the Center for Satellite Applications and Research (STAR) of the National Environmental Satellite, Data, and Information Service (NESDIS) for the National Oceanic and Atmospheric Administration (NOAA). The algorithm focuses on the Level 2A and Level 2B products, which process the raw input data from the Level 1B products generated by the Indian Space Research Organisation (ISRO).

## 1.2. Oceansat-3 (EOS-06) Mission

The Oceansat-3 (EOS-06) mission, launched by ISRO on November 26, 2022, is a follow-on mission to the Oceansat-2 and SCATSAT-1 missions. Oceansat-3 carries three key payloads: the Ocean Color Monitor (OCM-3), the Scatterometer (OSCAT-3), and the Sea Surface Temperature Monitor (SSTM-1). The OSCAT-3 is a microwave radar instrument specifically designed to measure ocean surface wind vectors. Compared to its predecessors, OSCAT and SCATSAT-1, OSCAT-3 offers enhanced features, including higher resolution and more comprehensive and accurate data. The sensor transmits and receives radar pulses using a conical scanning geometry, dual-polarization (vertical and horizontal), and a pencil-beam antenna, measuring the radar backscatter or  $\sigma^0$  at a  $58^\circ$  incidence angle for the outer beam vertical polarization and a  $49^\circ$  incidence angle for the inner beam horizontal polarization. A schematic of the OSCAT-3 measurement geometry is shown in Figure 1-1.

The swath of the OSCAT-3 measurements has a maximum extent of 1800 km (for the outer beam only). However, the measurement swath that includes both the outer and inner beams is reduced to 1400 km (see Figure 1-1). The  $\sigma^0$  measurement data are stored in a scan-by-scan mode in the Level 1B data. From the Level 1B data,  $\sigma^0$  is grouped into wind vector cells (WVC) with a nominal grid spacing of 12.5 km and 25 km, which are stored in the Level 2A data products. From the Level 2A data,  $\sigma^0$  is converted into wind speeds and wind directions for each WVC through the wind retrieval algorithm using an empirical Geophysical Model Function (GMF). The wind retrievals are stored in the Level 2B data products. From Level 2B, the swath-by-swath wind retrievals are further gridded into global winds product in Level 3.

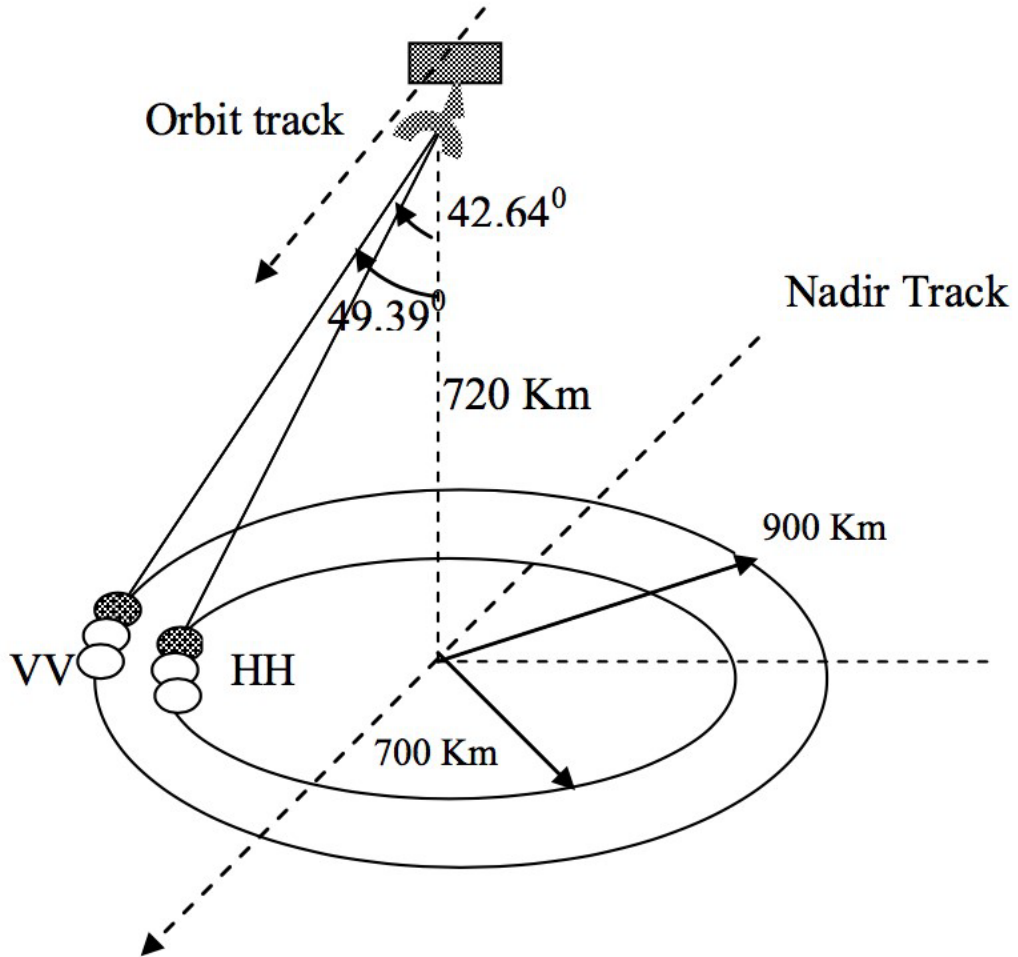


Figure 1-1 OSCAT-3 Measurement Geometry.

### 1.3. System Specifications

The OSCAT-3 offers many improvements over its predecessors, OSCAT and SCATSAT-1, including higher resolution as well as more comprehensive and accurate data. Table 1-1 outlines the key system parameters of OSCAT-3.

*Table 1-1. OSCAT-3 Specifications*

<b>Parameter</b>	<b>Inner Beam</b>	<b>Outer Beam</b>
Satellite Altitude	720 km (nominal)	
Frequency	Ku-band 13.51 GHz	
Wavelength	0.022 m	
Swath	1400 km	1800 km
Polarization	HH	VV
One Way 3dB Foot Print at Equator (Az x El)	29.5 km X 20 km	38 km X 22 km
Scan Rate	16 rpm	
Antenna Diameter	1.4 m	
Wind vector cell size	12.5 km X 12.5 km and 25 km X 25 km (LRScat) and 5 km X 5 km (HRScat)	

## 2. OSCAT-3 DATA PRODUCTS

The OSCAT-3 data products generated by ISRO are organized into three levels per half orbit: Level-1B, Level-2A and 2B. These products are produced separately for ascending (South Pole to North Pole, SN) and descending (North Pole to South Pole, NS) passes, with typically 14-15 orbits daily. Additionally, a Level-3 data product is generated on a daily basis. All product files from ISRO are provided in Hierarchical Data Format version 5 (HDF5) with the “.h5” file extension. Details about the formats of ISRO’s OSCAT-3 data files are provided in [1].

- Level-1B (L1B) contains sigma0 data at the slice and footprint levels, provided in a scan-by-scan format.
- Level-2A (L2A) is a gridded sigma0 product derived from L1B, organized into wind vector cells (WVC) with grid spacings of 12.5 km and 25 km.
- Level-2B (L2B) uses sigma0 data from L2A to produce wind retrievals for each WVC, stored with the same grid spacings of 12.5 km and 25 km.
- Finally, the Level-3 (L3) product combines global sigma0 and wind data into a daily global grid.

NOAA began receiving near real-time (NRT) data from ISRO indirectly through the STAR Central Data Repository (SCDR) in May 2023. The NESDIS/STAR Ocean Surface Winds Team (OSWT) utilized the L1B data to process its own versions of the L2A and L2B data at a 12.5 km grid spacing. Both L2A and L2B files are stored in HDF5 format. In addition to the ocean surface vector wind data, NOAA has generated a novel rain rate and rain-impact flag as supplementary information included in the L2B data product. The rain rate information required additional processing using Python. This L2B product with rain rate is stored in NetCDF format. However, we do not generate the L3 product. From this point onward, we’ll refer to NOAA’s L2A and L2B files simply as the L2A and L2B products.

### 2.1. File Naming Conventions

The L2A and L2B file naming conventions use the prefixes **NL2A125VHSL** and **NL2B125VHSL**, respectively, followed by the corresponding L1B filename from which the L2A and L2B files are derived.

The meaning of the prefix is the following:

**N** – Indicates a NOAA product

**L2A** or **L2B** – Indicates product type **125**

– Grid spacing for 12.5 km.

**VH** – Measurement Polarization: VH means V and H Pol.

**SL** – Utilizing slice sigma0

The meaning of the L1B file naming is the following:

**E06SCTL1BYYYYDDD\_AAAAA\_BBBBB\_ZZ\_yyyy-dddThh-mm-ss\_vx.x.x.h5**

**E06** – Stands for EOS-06 satellite.

**SCT** – Indicates scatterometer payload.

**L1B** – Indicates L1B product.

**YYYYDDD** – Indicates year and Julian of observation.

**AAAAA** – Starting orbit number.

**BBBBB** – Ending orbit number.

**ZZ** – Orbit direction; i.e. NS for descending or SN for ascending.

**yyyy-dddThh-mm-ss** – Year, Julian day, hours, minutes, seconds of product generation.

**vx.x.x** – Version number.

An example of the L1B and the corresponding L2A and L2B files are

L1B filename:

E06SCTL1B2024350\_10850\_10851\_NS\_2024-350T20-04-19\_v1.0.3.h5

L2A filename:

NL2A125VHSL\_E06SCTL1B2024350\_10850\_10851\_NS\_2024-350T20-0419\_v1.0.3.h5

L2B filename:

NL2B125VHSL\_E06SCTL1B2024350\_10850\_10851\_NS\_2024-350T20-04-19\_v1.0.3.h5

NL2B125VHSL\_E06SCTL1B2024350\_10850\_10851\_NS\_2024-350T20-0419\_v1.0.3.nc

Note: The difference between L2B files with the .h5 and .nc extensions is that the .h5 files contain wind data only, while the .nc files contain both wind and rain data.

### 3. LEVEL-2A (L2A)

The L1B product from ISRO is used to generate NOAA's Level-2A (L2A) product. The L2A product averages sigma0 measurements into swath grid cells, also referred to as wind vector cells (WVCs). The L2A data processing uses sigma0 slices from the L1B data, provided in a scan-by-scan mode and satellite ephemeris information to generate data at fixed grid intervals of 12.5 km or 25 km along and across the sub-satellite track, forming a gridded swath.

#### 3.1. Grid Cell Generation

In order to transform sigma0 from L1B in a scan-by-scan format into the gridded cell format in L2A we need to know precise ephemeris information along the scan. For each antenna scan, we use the satellite state vectors from the orbit and attitude (OAT) data in L1B data and interpolates the position and velocity vectors to each pulse along the scan for each antenna beam. Given the scan start time for each scan in the L1B data, we can determine the time of each pulse. OSCAT-3 has an antenna scan rate of 16 rpm. Since there are 361 pulses per scan for the outer beam and 360 pulses per scan for the inner beam, the rate of change along the scan equals  $60/16/361$  seconds per pulse for the outer beam and  $60/16/360$  seconds per pulse for the inner beam. Using the interpolated position and velocity for each pulse and each beam, we can compute orbital elements necessary to determine grid cell with respect to the satellite ground track. The orbital elements computed are semi-major axis, eccentricity, inclination, longitude of ascending node, argument of latitude and nodal period. In addition, the argument of latitude was taken to account for the location of the beams in the circular motion about the nadir using the following formulation

$$\Delta uu = WW/RR \cdot \cos(\omega\omega) \quad (3.1)$$

where,  $WW$  is the half scan width equals 918 km and 700 km for the outer beam and inner beam, respectively. The  $\omega\omega$  is the antenna azimuth angle in unit radians and the  $RR$  is Earth radius equals 6378.1363 km. And  $\Delta uu$  is a change in argument of latitude in unit radians with respect to argument of latitude,  $uu$ , at sub-satellite point. The effective argument of latitude then equals

$$uu_{pp} = uu + \Delta uu \quad (3.2)$$

where  $uu_{pp}$  is argument of latitude for each pulse. In (3.2), the  $uu$  and  $\Delta uu$  has been converted into unit degrees before summation. Next, using the orbital elements computed above, we then use it as inputs to calculate the grid cell associate with each of the L1B slice geolocations. The general idea of computing the grid cell associated with a given latitude and longitude is to calculate a relative distance parallel and perpendicular to the orbit. The grid cell index  $(ii, jj)$  can then be achieved by

$$ii = LL / 2\pi\pi \cdot NNNN \quad (3.3)$$

$$jj = \phi \cdot RR / GGGG + NNNN / 2 \quad (3.4)$$

Here,  $ii$  and  $jj$  are along (row) and across (column) track index, respectively. The  $NNNN$  is a number of maximum grid cells along track of one full orbit that is defined as 1624 for 25 km grid cell spacing or 3248 for 12.5 km grid cell spacing.  $RR$  is Earth radius.  $GGGG$  is grid size of 25 km or 12.5 km. Since a OSCAT-3 L1B file contains only a half orbit, the maximum number along track index is 812 and 1624, respectively. The  $NNNN$  is the number of grid cells across swath and equals 76 or 152 for 25 km or 12.5 km grid cell spacing, respectively. The  $LL$  and  $\phi$  are the along track and across track angles measured in radians. These two parameters can be achieved through a numerical method based on the Space Oblique Mercator transformation given by J. P. Snyder, "Map Projections Used by the U.S. Geological Survey," USGS Bulletin 1532 [2]. In addition, the  $LL$  parameter requires further modification so that it can be compatible with OSCAT-3 orbit definition that originates from the North Pole instead of from the Equator as defined by Snyder and half-orbit file instead of full-orbit file so that the  $ii = 1$  at the beginning of each half-orbit regardless of ascending or descending portions of the orbit. The modified  $LL$  are

$$LL = LL - \pi\pi/2, \quad \text{for ascending orbit} \quad (3.5)$$

$$LL = LL + \pi\pi/2, \quad \text{for descending orbit} \quad (3.6)$$

The  $jj$  index range is from 1-76 for 25km, and 1-152 for 12.5km and is numbered from right to left with respect to satellite heading North. For each pulse and each slice, the cell index ( $ii, jj$ ) keeps track of the number of sigma0 per cell and per row and the number of sigma0 per pulse per cell. This information will be used to group sigma0 of the same pulse within a grid cell.

Figure 3-1 illustrates row ( $i$ ) and cell ( $j$ ) index generations for 12.5 km from three nonconsecutive scans where the x-axis is the along scan azimuth (0-360 degrees), the thin overlapping bell-shaped curves correspond to the cell index (left y-axis), and the thick curves correspond to the row index (right y-axis).

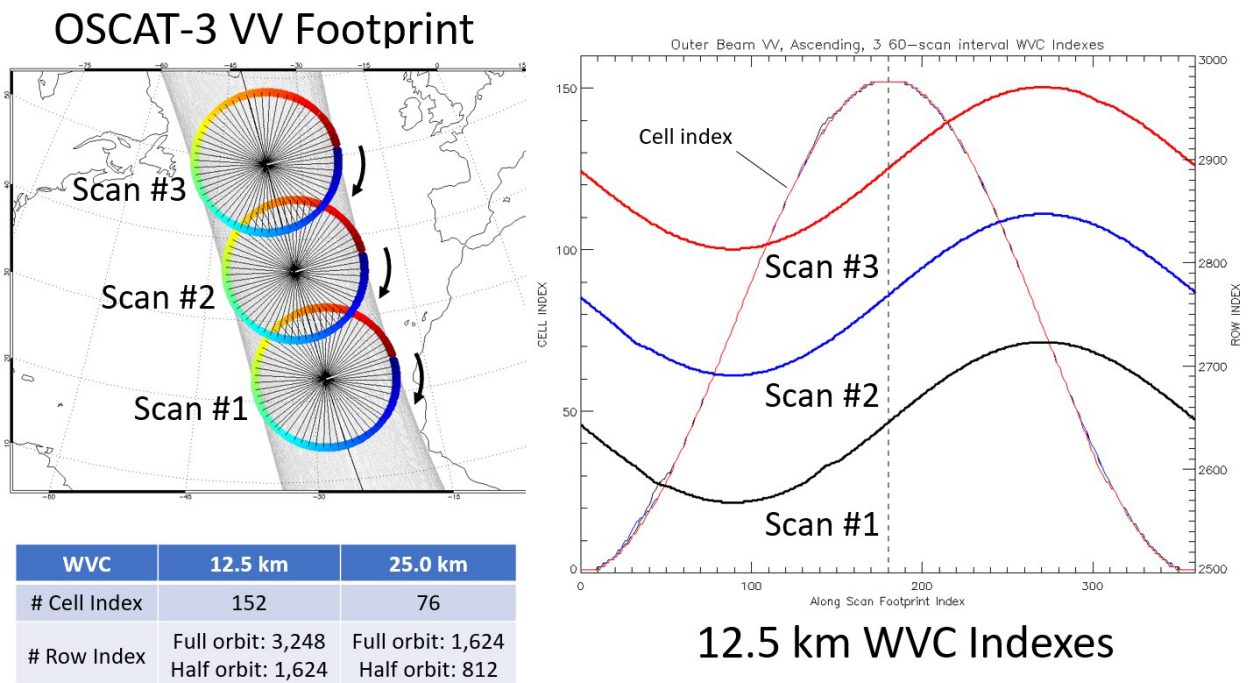


Figure 3-1. L2A row and cell index generation.

## 3.2. Sigma0 Grouping

A scheme for sigma0 grouping or compositing sigma0 is depicted in Figure 3-2. The sigma0 composite is performed per beam, per pulse, and per grid cell. In Figure 3-2, the grid cell, as defined in the previous section, is shown by the thick black grid lines of a chosen grid size. In OSCAT-3 L2A processing, we use grid size of 12.5 km; however, larger grid sizes of 25km and 50 km can also be used. Within each grid cell, the slice parameters belonging to a single pulse are grouped together, as depicted by the rectangular boxes in Figure 3-2. Also, in Figure 3-2, the shorter ellipse represents an inner beam pulse footprint, and the longer ellipse represents an outer beam pulse footprint. Finally, the resulting composite sigma0 is shown in the bottom row of Figure 3-2.

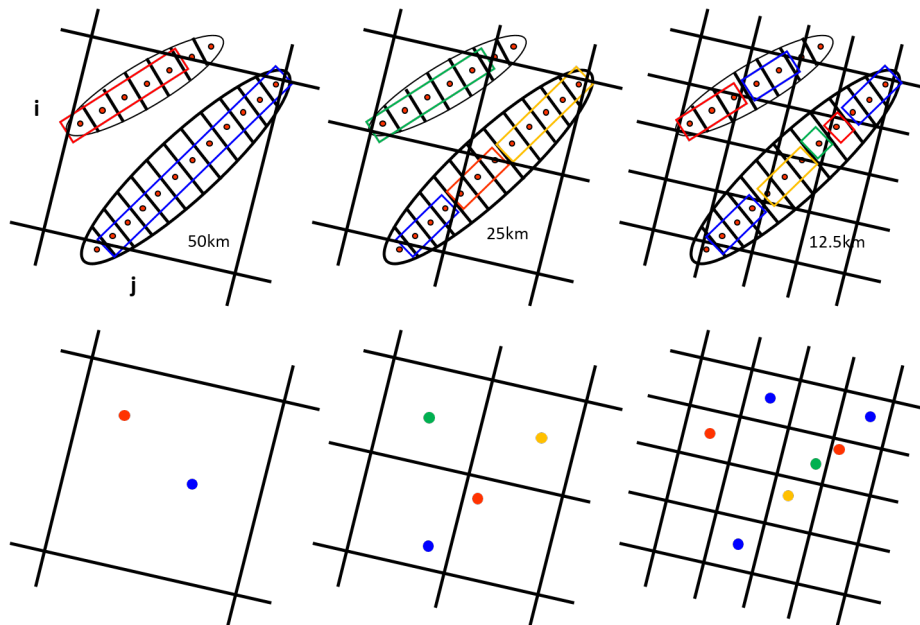


Figure 3-2. Sigma0 compositing scheme.

The composite sigma0 and their associate parameters are computed by the following method. Composite latitude and longitude are the average of the individual slice latitudes and longitudes as

$$LLLLLLccccpp = (\sum_{NNss=1}^{NN} LLLLLLssssscss) / NN \quad (3.7)$$

$$LLLLLLccccpp = (\sum_{NNss=1}^{NN} LLLLLLssssscss) / NN \quad (3.8)$$

where  $NN$  is the number of slices within a wind vector cell. For the other parameters, a weighted average by X-factor has been applied. The weighted factor is computed by

$$\begin{aligned} XX_{tccttss} &= \sum_{ss=1}^{NN} XX_{ssssscss} \\ XX_{ww} &= XX_{ssssscss} / XX_{tccttss} \end{aligned} \quad (3.9)$$

$$(3.10)$$

In (3.9) and (3.10), the weighted factor has done in a normal unit (non-dB). The other composite parameters including signal-to-noise ratio and brightness temperature ( $T_b$ ) are then computed by the follow

$$\sigma\sigma_{ccc0pp} = \sum_{NNss=1}^{NN} XX_{ww} \cdot \sigma\sigma_{ssss0ccss} \quad (3.11)$$

$$GGNNRR_{ccc0pp} = \sigma\sigma_{ccc0pp} / (\sum_{NNss=1}^{NN} XX_{ww} \cdot \sigma\sigma_{ssss0ccss} / GGNNRR_{ssssccss}) \quad (3.12)$$

$$\theta\theta_{ccccpp} = \sum_{ss=1}^{NN} XX_{ww} \cdot \theta\theta_{ssssccss} \quad (3.13)$$

$$\varphi\varphi_{ccccpp} = \sum_{ss=1}^{NN} XX_{ww} \cdot \varphi\varphi_{ssssccss} \quad (3.14)$$

$$TTTT_{ccccpp} = \sum_{ss=1}^{NN} XX_{ww} \cdot TTTT_{ssssccss} \quad (3.15)$$

In (3.11) the slice sigma0 was converted from dB into normal units and the sigma0 was assigned a negative sign based on the negative sigma0 flag before computing the composite sigma0. The composite signal-to-noise ratio (SNR), incidence angle, azimuth angle and brightness temperature are computed in (3.12) – (3.15) respectively. In addition to composite parameters, the composite sigma0 quality flag was based on the slice sigma0 quality flag. If one of the slice sigma0 was flagged, then the composite sigma0 was also flagged. There is an exception for the negative sigma0 flag (bit9), where the flag was set based on the sign of the resulting composite sigma0 sign. Finally, the sigma0 (3.11) and

SNR (3.12) are converted back to dB unit. In addition to the above parameters, the  $K_p$  coefficients was carried along from L1B in to L2A by similar weighted averaging as in (3.11) for  $K_{pa}$ ,  $K_{pb}$  and  $K_{pc}$ . A complete list of L2A parameter and range of value can be found in Appendix A.

Figure 3-3 shows an example of one-half orbit of L2A slice composite at 12.5 km WVC swath grid resolution. The color code represents the number of composite sigma0 values per WVC. Two overlapping swaths from the outer and inner beams can be seen, with high concentrations of sigma0 counts at the edges of swaths.

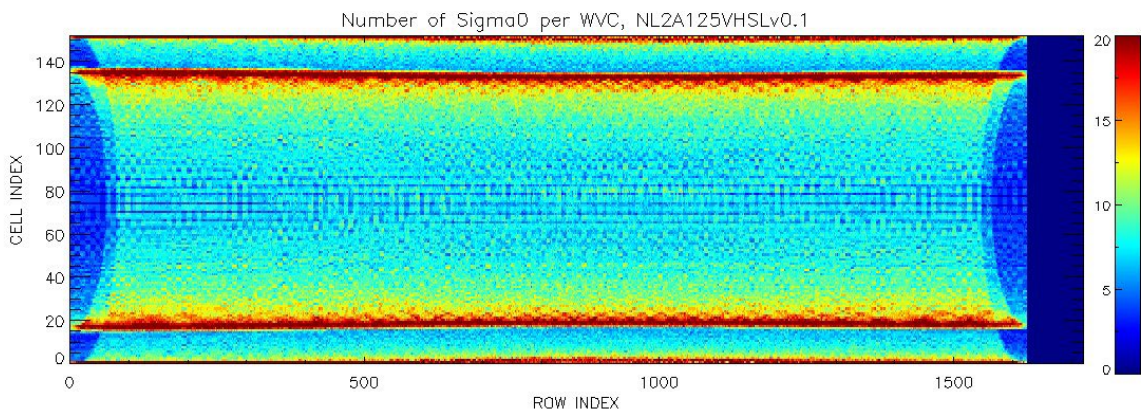


*Figure 3-3. Sigma0 slice composite counts per 12.5 km WVC.*

Figure 3-4 shows an example of a OSCAT-3 ascending pass of 12.5 km sigma0 composites from fore-look VV, aft-look VV, fore-look HH, and aft-look HH (so called the four flavors of sigma0).

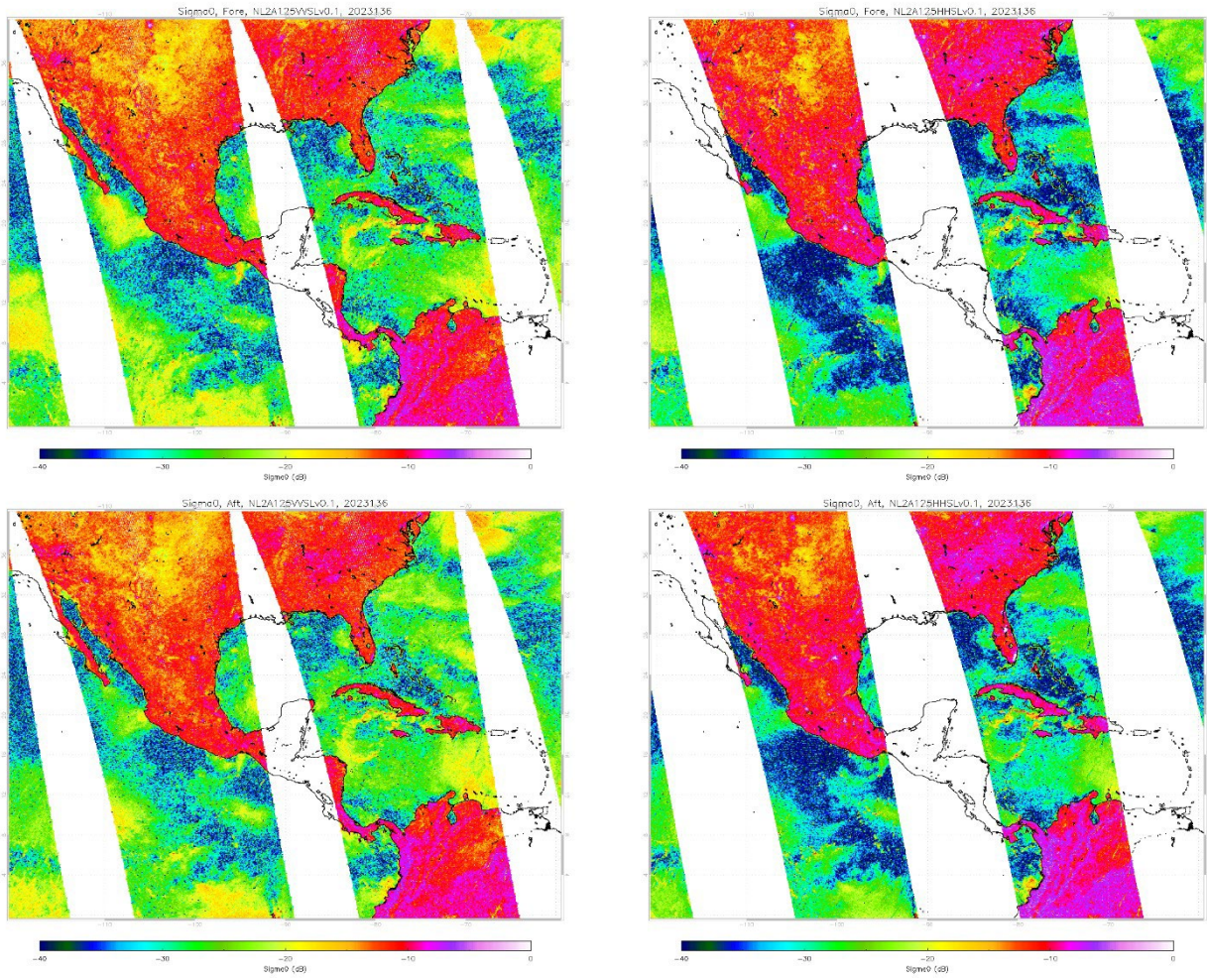


Figure 3-4. Slice composite of four-flavors  $\sigma_0$ .

### 3.3. Row Time

Finally, the last parameter we derived for L2A is the time stamp. Since the time stamp from L1B is given as the beginning of each scan, we need to convert those times into a time at a given row in L2A. The wind vector cell row time is derived by

$$TT_{ss} = rr \cdot ii / (0.5 \cdot NNNN) + LL_0 \quad (3.16)$$

$rr$  is time difference between the last scan and the first scan,  $LL_0$  in the L1B half-orbit.  $ii$  is the along track index or row index,  $NNNN$  is number of full-orbit grid cell which are 1624 for 25 km and 3248 for 12.5 km, and  $TT_{ss}$  is the time in second at row index  $ii$ . The row time in (3.16) is stored in seconds from 1 January 2000, 00:00 UTC.

## 4. LEVEL-2B (L2B)

The OSCAT3 wind vector data is generated at Level 2B. Using the swath grid cell  $\sigma_0$  measurements from Level 2A, wind retrievals are produced at a grid cell resolution of 12.5 km. For each grid cell, wind speed and wind direction are determined through a wind inversion process based on maximum likelihood estimation (MLE) using the Geophysical Model Function (GMF). The Level 2B (L2B) data product is created for each half-orbit, corresponding to L2A 12.5 km grid described in the previous section.

The generation of the L2B product involves three main components. The first is the preprocessing step, where  $\sigma_0$  values are prepared for wind inversion. This includes applying two-way atmospheric attenuation corrections and  $\sigma_0$  calibration. A land mask is also applied at this stage to distinguish between land and ocean points.

The second step is the wind inversion algorithm, where  $\sigma_0$  measurements are converted into wind vector solutions. Since the GMF is nonlinear, this process produces multiple wind vector solutions, known as ambiguities.

The third step involves an ambiguity removal process to select the unique wind solution.

Additionally, a new rain rate and rain impact rain flagging algorithm is implemented after the generation of wind retrievals to identify those potentially affected by rainfall. The final L2B data output is then saved in a NetCDF file.

The three main components and the rain rate estimation process from OSCAT3 are described in further detail below.

### 4.1. Preprocessing

An L2A 12.5km half-orbit file contains 1,624 WVCs along the track and 152 WVCs across the track. As each WVC is processed, the individual composite  $\sigma_0$  values are evaluated for wind retrieval usability utilizing the L2A  $\sigma_0$  quality flags. Additionally, a land mask map with a resolution of approximately 0.1 degrees is used to identify samples corresponding to ocean points.

The latitude and longitude centroids of each WVC are determined in this step by averaging the valid ocean points' composite latitude and longitude values. The number of valid composite sigma0 measurements per WVC is saved for use later in the wind inversion process. During this preprocessing, sigma0 calibration is applied, as describe below.

### 4.1.1. Sigma0 Calibration

Before composite sigma0 ( $\sigma^0$ ) can be used for wind inversion, it must first be corrected for atmospheric effects and calibrated with respect to the GMF. The measured  $\sigma^0$  is corrected for atmospheric attenuation as

$$\sigma_{\sigma_{SSSSSSS}}^0 = \sigma^0 \cdot NNTTAA / \cos(\theta\theta) \quad (4.1)$$

Here,  $NNTTAA$  represents the interpolated two-way atmospheric attenuation derived from a global monthly atmospheric attenuation climatology developed by F.J. Wentz (1995) [3]. The  $\theta\theta$  is the composite incidence angle from L2A. The result,  $\sigma_{\sigma_{SSSSSSS}}^0$ , is the sigma0 value corrected for atmospheric attenuation at the surface.

Using  $\sigma_{\sigma_{SSSSSSS}}^0$ , calibration correction values are applied for polarization (V-pol and H-pol) The calibrated sigma0 is computed for each beam as

$$\sigma_{\sigma_{ww0SS}} = \sigma_{\sigma_{SSSSSSSS0}} - \Delta\sigma\sigma^0 \quad (4.2)$$

Here,  $\sigma_{\sigma_{ww0SS}}$  represents the corrected sigma0 for each polarization (V-pol or H-pol), which will be used in the wind inversion step, and  $\Delta\sigma\sigma^0$  represents the sigma0 calibration values, which have gradually changed over time, as shown in Figure 4-1. In (4.2), the sigma0 calibration is applied in dB units.

Initially, when  $\Delta\sigma\sigma^0$  was determined based on September 2023 data, the values were 0 dB for V-pol and -0.65 dB for H-pol. As of this writing, the calibration values based on August 2024 data were used, showing that sigma0 had drifted -0.22 dB lower. Consequently, the revised calibration values are -0.22 dB for V-pol and -0.88 dB for H-pol.

## OSCAT3 Sigma0 Calibrations

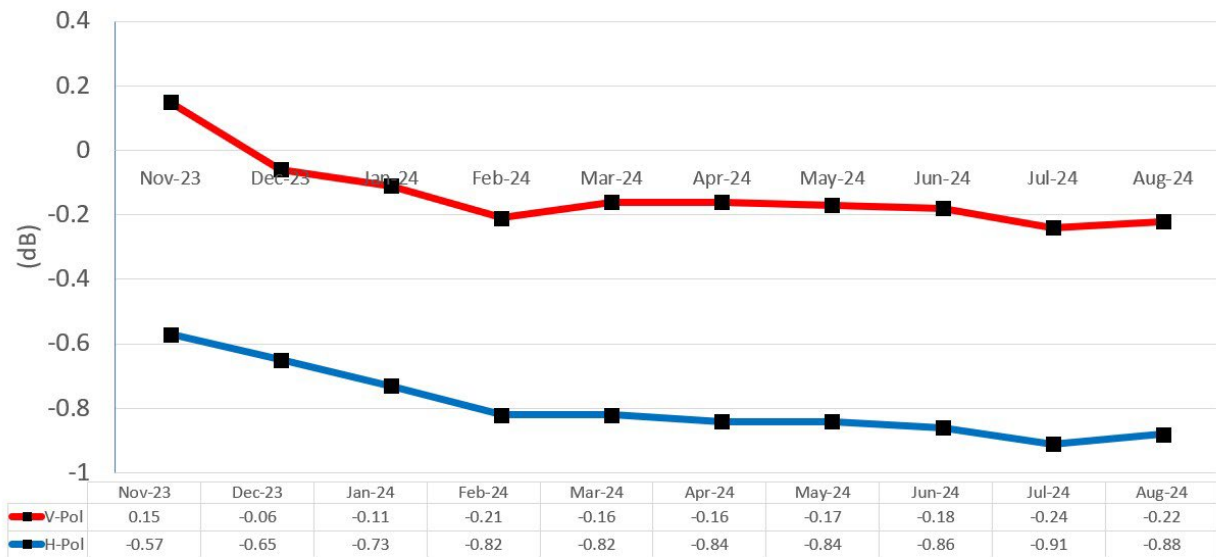


*Figure 4-1. Changes in sigma0 calibration values over time.*

### 4.2. Wind Inversion

The gridded composite sigma0 values are utilized to derive wind speed and direction through the Maximum Likelihood Estimation (MLE) approach, which minimizes the difference between the measured  $\sigma^0$  and predicted  $\sigma^0$  computed from the Geophysical Model Function (GMF). Details of the GMF used in this process are described in the next section. The MLE objective function is expressed as

$$LLT_jj = -\sum_{N_{ss}=1} (\frac{\sigma_{\sigma i i 0} - v_{v t t} S S G G G G G G i i}{\sigma_{\sigma i i 0} - v_{v t t} S S G G G G G G i i})^2 \quad (4.3)$$

where  $\sigma^0$  represents the calibrated sigma0 from (4.2) within a given wind vector cell (WVC); and  $N$  is the number of valid sigma0 determined during the preprocessing step. The negative sign in the right side of (4.3) indicates that the objective function's maximum value

corresponds to the minimum sigma0 difference between the measured and predicted.  $var$  denotes the variance of  $\sigma^0$ .

Wind speed solutions are determined by stepping through wind directions in 2.5-degree increments. For each wind direction, the wind speed that maximizes the objective function is identified, resulting in a total of 144 wind speed and direction pairs.

Typically, the objective function yields up to four local maxima. The wind speeds and directions corresponding to these maxima are referred to as ambiguities. When all 144 solutions are retained, the approach is called the Multi-Solution Scheme (MSS). Both the four-ambiguity approach and the 144 solutions approach play important roles in determining the unique solutions for the final outputs of the L2B product. The process of selecting the unique wind vector solution is described in the ambiguity removal section.

#### 4.2.1. Geophysical Model Function

The Geophysical Model Function (GMF) used in OSCAT3 retrievals is the same as SCATSAT-1 GMF, which was developed based on the NSCAT4 GMF [4-5]. The GMF can generally be expressed in the following form:

$$GGAAGG = NN_0[1 + NN_1 \cos(\emptyset) + NN_2 \cos(\emptyset)] \quad (4.4)$$

where  $\emptyset$  represents the relative wind direction, and the  $A$  coefficients depend on both wind speed and incidence angle.  $A_0$  is a first-order term dependent on wind speed, while the higher-order harmonics ( $A_1$  and  $A_2$ ) determine the wind direction characteristics.

The  $A_0$  term in the NSCAT4 GMF [4-5] has been modified so that its trend at high winds aligns with measurements obtained from aircraft measurements. These measurements were made using the IWRAP radar system [6] on the NOAA P-3 aircraft. This modified version of the NSCAT4 GMF is referred to as NSCAT4.H [7], and it has been employed in both SCATSAT-1 and OSCAT3 wind retrievals.

#### 4.2.2. Solution Ranking

As mentioned earlier, the wind solutions usually result in up to 4 ambiguities, which are associated with the maxima of the objective function defined in (4.3). Using 2.5-degree increments for wind directions during the wind speed search process results in 144 pairs of wind speeds and directions, along with 144 residuals calculated from (4.3), referred to as the MLE values.

Initially the four ambiguities correspond to the highest four MLE values among these 144 solutions. These initial ambiguities are further refined to more precise values using an interpolation method. After refinement, ambiguities are sorted and ranked based on their MLE values; with the highest MLE assigned the first rank, the second-highest assigned the second rank, and so on. These four refined ambiguities are then saved for further processing before being included in the final L2B data output.

### **4.3. Ambiguity Removal**

To determine a unique wind vector from the set of ambiguity solutions, a procedure known as ambiguity removal processing is implemented. Several approaches are utilized for ambiguity removal in scatterometer wind retrievals. In OSCAT3 ambiguity removal, we employ a combination of Multi-Solution Scheme (MSS), Direction Interval Retrieval with Thresholded Nudging (DIRTH) [8], and a Variational Data Assimilation (VAR) approach. This methodology ensures a meteorologically consistent wind field while avoiding excessive smoothing of the retrieved wind field. A schematic of the ambiguity removal process is shown in Figure 4-2.

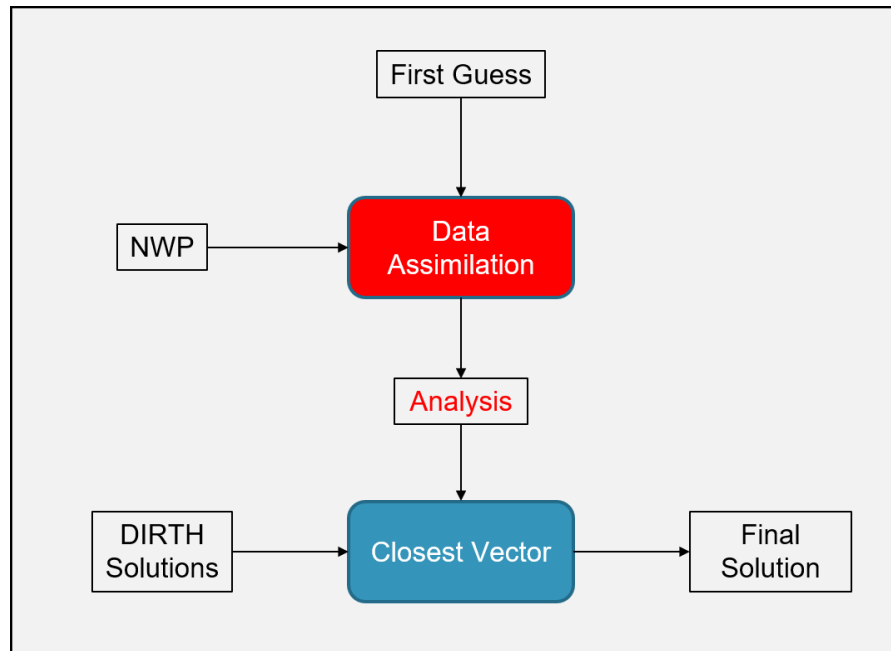


Figure 4-2. Ambiguity removal scheme.

(4.5)

In variation data assimilation, the objective is to find assimilated wind solutions that maximize the conditional probability of model winds,  $x$ , given observation winds,  $y$ , denoted as  $p(x|y)$ . Using Bayes' theorem and assuming Gaussian noise statistics for both the model and observations,  $p(x|y)$  can be expressed as

$$p(x|y) = c \cdot e^{-\frac{1}{2} \frac{(x-x_0)^2}{\sigma_y^2}} \cdot e^{-\frac{1}{2} \frac{(y-xx)^2}{\sigma_0^2}} \quad (4.5)$$

Here,  $x$  represents the model winds with a probability distribution  $p(x)$ , and  $y$  represents the scatterometer winds with a probability distribution  $p(y)$ .  $\sigma_0$  and  $\sigma_y$  are the variances of the model and observations, respectively, while  $x_0$  represents the mean model winds.

When considering the model and measured wind fields, the variational data assimilation method is referred to as 2DVAR because it handles two-dimensional data. However, to simplify the solution, each wind vector is treated independently instead of analyzing the entire wind field; this is referred to as 1DVAR. With the 1DVAR approach, the log likelihood of (4.5) is simplified to

$$JJ(x) = \frac{1}{2} \frac{(y - x)^2}{\sigma_y^2} + \frac{1}{2} \frac{x^2}{\sigma_0^2} \tag{4.6}$$

To solve for  $x$  that minimizes the errors in (4.6), we compute

$$\frac{\partial JJ(x)}{\partial x} = 0 \tag{4.7}$$

$$\frac{\partial}{\partial x} \left( \frac{(y - x)^2}{\sigma_y^2} + \frac{x^2}{\sigma_0^2} \right) = 0$$

The solution of the assimilated wind value  $x_{\bar{x}}$ , called the *analysis*, can be expressed as

$$x\bar{x} = \frac{\sigma_0^2 + \sigma_y^2}{\sigma_0^2 + \sigma_y^2} x x_0 + \frac{\sigma_0^2}{\sigma_0^2 + \sigma_y^2} (y y - x x_0) \quad (4.8)$$

The analysis winds from (4.8) can be rewritten in the form

$$x\bar{x} = x x_0 + K K (y y - x x_0) \quad (4.9)$$

Here,  $K$ , commonly known as the Kalman filter, is given by

$$K = \frac{\sigma_0^2}{\sigma_0^2 + \sigma_y^2} \leq 1 \quad (4.10)$$

To derive the analysis wind in OSCAT3, the NCEP Numerical Weather Prediction (NWP) model and initial guess wind vectors from OSCAT3 retrievals are utilized, as shown in Figure 4-2. As discussed in the previous section, wind inversion produces 144 pairs of wind speeds and directions (MSS). The initial OSCAT3 wind vectors are selected from the MSS vectors based on the smallest difference (closest) between these vectors and the collocated NWP.

Since MSS wind direction range from 0 to 360 degrees in 2.5-degree increments, selecting initial OSCAT3 wind vectors directly from the MSS solutions would result in an overly smooth wind field. To address this, the Direction Interval Retrieval with Thresholded Nudging (DIRTH) [8] method was implemented to filter the MSS solutions and restrict the possible range of wind directions used. These filtered MSS solutions are referred to as DIRTH solutions. The range of DIRTH wind directions depends on the shape of the

MLEwind direction function distribution and the DIRTH threshold value, which can range from 0% to 100%. If the full 0-360 degree range of wind directions is used, the DIRTH threshold is set to 100%, which is equivalent to the MSS solutions. Ultimately, the initial OSCAT3 wind vectors are selected based on the smallest difference between the DIRTH solutions with an 80% threshold and the NWP to determine the analysis wind.

Once the analysis winds have been derived, a unique wind vector solution is selected based on the smallest difference between the DIRTH solutions (with 80% threshold) and the analysis winds as shown in Figure 4-2. These selected solutions are the final OSCAT3 wind retrievals. Note that the final solution will have a 2.5-degree increment since it was selected from the DIRTH solutions. The original refined 4 ambiguities derived previously are retained; however, one of the 4 ambiguities is overwritten by this unique DIRTH solution. The ambiguity that was overwritten is selected based on the smallest difference (closest) between the 4 ambiguities and the unique DIRTH solution.

#### 4.4. Rain-impacted Wind Retrievals

The performance of scatterometer winds can be adversely impacted in the presence of rainfall, especially since OSCAT-3 operates at a higher frequency in the Ku-band. Rain induced sigma0 measurements will lead to erroneous wind retrievals if not properly flagged or corrected. Although OSCAT-3 was not originally designed to measure rainfall intensity, it is possible to estimate OSCAT-3 rain rates using supervised machine learning algorithm.

In addition to sigma0 measurements, OSCAT-3 simultaneously measures brightness temperature ( $T_b$ ) through its noise channels. While OSCAT-3 is not designed as a radiometer, the  $T_b$  measurements, combined with wind retrievals and ancillary sea surface temperature (SST) data from a Numerical Prediction Model (NWP) model, provide sufficient information to estimation rain rates through machine learning predictions.

The specific machine learning algorithm used for OSCAT-3 rain rates estimation is the Support Vector Machine (SVM), implemented using the Python scikit-learn library. The SVM model was trained on features derived from a combination of brightness temperatures ( $T_b$ ), NWP SST, and OSCAT-3 retrieved wind speeds. The training rain rate targets were obtained from GPM microwave Imager (GMI) measurements [9] collocated within a 30-minute time window of OSCAT-3 passes.

## 4.4.1. Rain Rate and Rain Flag.

Details of the rain rate model development are provided in [10]. The inputs to the rain rate model include the estimated atmospheric transmissivities ( $\tau$ ), as expressed in (4.11), and the rain-impacted OSCAT-3 retrieved wind speed.

$$\tau \cong 1 - \frac{T_B}{GGGGTT} \quad (4.11)$$

In (4.11), the brightness temperature ( $T_b$ ) represents the average composite  $T_b$  measurements for each beam per WVC., while the sea surface temperature (SST) is derived from collocated NWP models.

Initially, the rain rate model [10] was developed using OSCAT3 data from August 2023. However, OSCAT3 brightness temperature measurements changed significantly between November 2023 and December 2023, as shown in Figure 4-3. This change impacted OSCAT-3 rain rate estimations, leading to underestimate of rain rates. Consequently, using August 2024 data, (4.11) was adjusted to account for this change by correcting the atmospheric transmissivities ( $\tau$ ) for V-pol and H-pol as follows

$$\tau_{VV} = 1 - \frac{T_{BB} + 32.8}{GGGGTT} \quad (4.12a)$$

$$\tau_{HH} = 1 - \frac{T_{BB} + 30.7}{GGGGTT} \quad (4.12b)$$

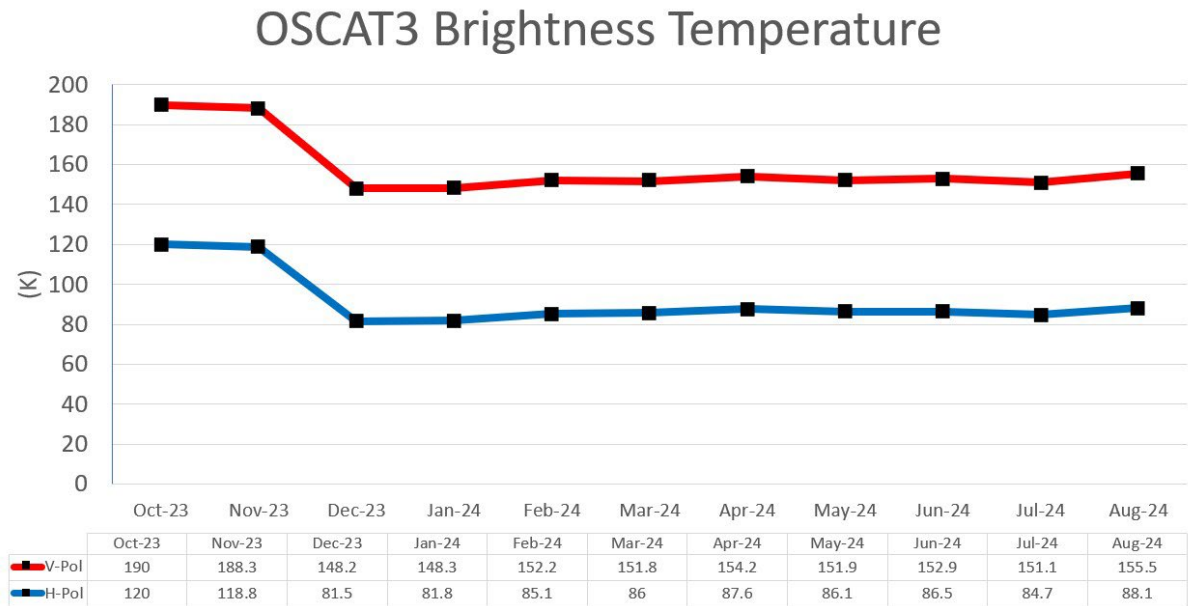


Figure 4-3. Changes in brightness temperature values over time.

Figure 4-4 shows OSCAT-3 wind speed performance with respect to GDAS in a presence of varying rainfall intensities, as derived from OSCAT-3 rain rate estimates. The rain rate retrievals are recommended for use only when the rain rate exceeds 1.5 mm/hr, as lower rain rates tend to be too noisy.

In mitigate the impact of rain on wind retrievals, a rain flag is applied based on OSCAT-3 rain rate estimates. The flag is activated when the rain rate exceeds 1.5 mm/hr and deactivated when rain rate falls below 1.5 mm/hr.

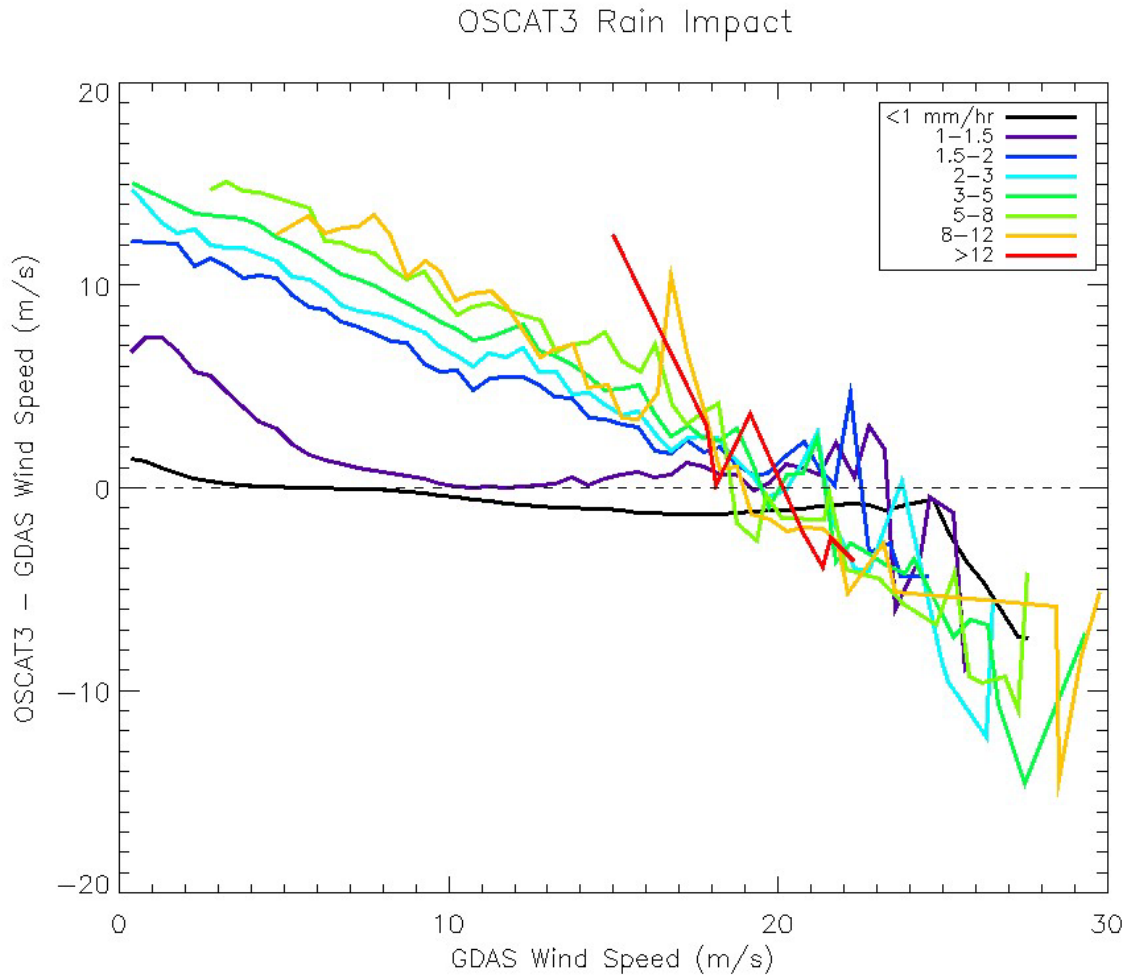


Figure 4-4. OSCAT-3 rain rates and rain impact on wind speed performance.

## 4.5. Quality Control

A list of L2B quality flags and their bit definitions is provided in Appendix B. Below is a brief description of each quality flag.

- **Invalid Sigma0**

This flag indicates whether there is valid sigma0 in the wind vector cell for further processing. The number of valid sigma0 in the wind vector cell is derived from L2A data.

- **Invalid model winds**

This flag checks for a valid model winds that are interpolated to the wind vector cells. If the model wind is available and they are not land or ice contaminated then they will be valid.

- **Land flag by model winds**

Land indicated by the model winds is indicate in this land flag.

- **Ice flag by model winds**

Ice indicated by the model winds is indicate in this ice flag.

- **Land flag**

The land flag reports in the L2B quality flag here comes from the land mask.

- **Ice flag**

The ice flag is set based on the ice flag from the L2A sigma0 quality flag, which was derived from the L1B sigma0 quality flag.

- **Invalid ocean sigma0 flag**

This flag checks for a valid ocean sigma0 flag. If either the land or the ice flag is set, then this flag is set.

- **Azimuth diversity flag**

The azimuth diversity flag check number of azimuth diversity in each WVC. If Sigma0 measurement flavors are 2 or less, then the flag is set.

- **Inversion attempt flag**

This flag is used to verify if sigma0 is valid before it can be used in the inversion process. If this flag is not set, there will be no inversion attempted.

- **Inversion invalid flag**  
After the sigma0 enter in the wind inversion process, if the wind inversion is not successful then this flag is set.
- **NOAA overall flag**  
The NOAA overall flag is use to summarize other quality flags. If one of the following flags is set; invalid sigma0, invalid ocean sigma0, inversion invalid, invalid model winds; then the NOAA overall flag will be set.
- **Rain flag usable flag**  
This flag is intended to identify parameters necessary to perform the rain rate retrievals. In OSCAT3 case, if there are available measurements from both V-pol and H-pol transmissivity and wind retrievals then rain flag is usable.
- **Rain flag**  
Rain flag is based on OSCAT3 rain rate retrievals. The rain flag is set if OSCAT-3 rain rate is greater than 1.5 mm/hr.

## 5. REFERENCES

- [1]. Microwave Data Processing Division, Signal and Image Processing Group, Space Applications Center, *Formats for EOS-06 Scatterometer Data Products*, E06/SCAT/DPFORMAT-DOC/1.0/SEP2022, Ahmedabad, India, 2022.
- [2]. J. P. Snyder, "Map Projections Used by the U.S. Geological Survey," USGS Bulletin 1532.

- [3]. F. J. Wentz, "Climatology of 14-GHz Atmospheric Attenuation," Remote Sensing Systems, September 30, 1995.
- [4]. F. J. Wentz and D. K. Smith, "A model function for the ocean normalized radar cross section at 14 GHz derived from NSCAT observations," *J. Geophys. Res.*, vol. 104, no. C5, pp. 11499-11514, 1999.
- [5]. KNMI Scatterometer Team, "NSCAT-4 Geophysical Model Function," [http://projects.knmi.nl/scatterometer/nscat\\_gmf/](http://projects.knmi.nl/scatterometer/nscat_gmf/)
- [6]. J. Sapp, P. Chang, Z. Jelenak, S. Frasier, and T. Hartley, "Sea-surface NRCS observations in high winds at low incidence angles," in Geoscience and Remote Sensing Symposium (IGARSS), 2015 IEEE International, Milan, Italy, 2015, pp. 1199–1202, doi: 10.1109/IGARSS.2015.7325987.
- [7]. S. Soisuvam, Z. Jelenak, P. Chang, J. Park, Q. Zhu, J. Sapp and F. Said, "Scatsat-1 High Winds Geophysical Model Function and Its Winds Application in Operational Marine Forecasting and Warning," IGARSS 2020.
- [8]. B. W. Stiles, B. D. Pollard and R. S. Dunbar, "Direction interval retrieval with thresholded nudging: a method for improving the accuracy of QuikSCAT winds," in *IEEE Transactions on Geoscience and Remote Sensing*, vol. 40, no. 1, pp. 79-89, Jan. 2002, doi: 10.1109/36.981351.
- [9]. Wentz, F.J., T. Meissner, J. Scott, K.A. Hilburn, 2015: Remote Sensing Systems GPM GMI Daily Environmental Suite on 0.25 deg grid, Version 8.2, Remote Sensing Systems, Santa Rosa, CA. Available online at [www.remss.com/missions/gmi](http://www.remss.com/missions/gmi).
- [10]. S. Soisuvam, Z. Jelenak, P. S. Chang and Q. Zhu, "A Machine Learning-Based Rain Rate Estimation from the OceanSat-3 Scatterometer Measurements," *IGARSS 2024 - 2024 IEEE International Geoscience and Remote Sensing Symposium*, Athens, Greece, 2024, pp. 5827-5830, doi: 10.1109/IGARSS53475.2024.10641001.

## 6. APPENDIX A

*Table 6-1. List of L2A HDF5 variables*

<b>Variable Name</b>	<b>Data Type</b>	<b>Dimensions</b>
azimuth_angle	float	1720 x 3500
brightness temperature	float	1720 x 3500
cell_index	int	1720 x 3500
incidence_angle	float	1720 x 3500
latitude_footprint	float	1720 x 3500
longitude_footprint	float	1720 x 3500
num_sigma0_per_cell	int	1720 x 152
num_sigma0_per_row	int	1720
row_index	int	1720
sigma0	float	1720 x 3500
sigma0_quality_flag	float	1720 x 3500
snr	float	1720 x 3500
wvc_row_time	string	1720

*Table 6-2. List of L2B NetCDF variables*

<b>Variable Name</b>	<b>Data Type</b>	<b>Dimensions</b>	<b>Description</b>
wspeeds	float	1720 x 152 x 4	Wind speed ambiguities
wdirs	float	1720 x 152 x 4	Wind direction ambiguities
mles	float	1720 x 152 x 4	MLE ambiguities
lat	float	1720 x 152	Latitude
lon	float	1720 x 152	Longitude
speed	float	1720 x 152	Selected wind speed
dir	float	1720 x 152	Selected wind direction
mle	float	1720 x 152	Selected MLE
Mspeed	float	1720 x 152	Model wind speed
Mdir	float	1720 x 152	Model wind direction
sst	float	1720 x 152	Model SST
rainrate	float	1720 x 152	Rain rate
txv	float	1720 x 152	V-pol transmissivity
txh	float	1720 x 152	H-pol transmissivity
ambiguity_select	short	1720 x 152	Selected ambiguity index
num_ambiguity	short	1720 x 152	Number of ambiguities
time	double	1720 x 152	Seconds since 1/1/2000 00 UTC
qc_flag	uint	1720 x 152	Quality Flag

## 7. APPENDIX B

*Table 7-1. L2A quality control flag.*

<b>Bit No.</b>	<b>Equal to 0 when</b>	<b>Equal to 1 when</b>
0	DES	ASC
1	HH	VV
2	AFT	FORE
3	Sea	Land
4	Good sigma0 (summary)	Poor sigma0 (summary)
5	Valid sigma0 (summary)	Invalid sigma0 (summary)
6	Good BT	Poor BT
7	Valid BT	Invalid BT
8	No land-sea boundary	Land-sea boundary
9	+ve sigma0	-ve sigma0
10	-	-
11	-	-
12	-	-
13	No ice	Ice
14	Data available at a given latitude-longitude for seaice flagging process	Missing data at a given latitude-longitude for seaice flagging process

	for 2 or more number of days	for 2 or more number of days
15	No ice-ocean contamination	Ice-ocean contamination

*Table 7-2. L2B quality control flag.*

<b>Bit No.</b>	<b>Equal to 0 when</b>	<b>Equal to 1 when</b>
0	Sigma0 is valid	Sigma0 is invalid
1	Model winds is valid	Model winds is invalid
2	Land is not detected by model winds	Land is detected by model winds
3	Ice is not detected by model winds	Ice is detected by model winds
4	Open ocean sigma0 is valid	Open ocean sigma0 is invalid
5	Land contamination is not detected in land mask	Land contamination is detected in land mask

6	Ice contamination is not detected by sigma0 flag	Ice contamination is detected by sigma0 flag
7	Sigma0 flavors are 2 or less	Sigma0 flavors are more than 2
8	Winds inversion is successful	Winds inversion is not successful
9	NOAA overall quality flag is not detected	NOAA overall quality flag is detected
10	Winds inversion is not attempted	Winds inversion is attempted
11	Rain flag is not usable	Rain flag is usable
12	Rain is not detected (rain rate < 1.5 mm/hr)	Rain is detected (rain rate > 1.5 mm/hr)
13	-	-
14	-	-
15	-	-

---

END OF DOCUMENT